ADVANCED FUNCTIONAL MATERIALS
www.afm-journal.de

Direct Arylation Polycondensation: A Promising Method for the Synthesis of Highly Pure, High-Molecular-Weight Conjugated Polymers Needed for Improving the Performance of Organic Photovoltaics

*Junpei Kuwabara, Takeshi Yasuda, Seong Jib Choi, Wei Lu, Koutarou Yamazaki, Shigehiro Kagaya, Liyuan Han, and Takaki Kanbara**

Alternating conjugated polymers of ethylenedioxythiophene and fluorene are prepared using three different synthetic methods to investigate the effects of these synthetic methods on the purity, field-effect transistor (FET) performance, and organic photovoltaic (OPV) performance of the polymer. In this study, microwave-assisted direct arylation polycondensation is used to obtain a high-purity, high-molecular-weight (147 kDa) polymer. This pure polymer exhibits a high FET hole mobility of 1.2×10^{-3} cm^2 V^{-1} s^{-1} and high OPV performance with a power conversion efficiency of 4%, even though the polymer forms an amorphous film, which absorbs in a limited region of the spectrum.

1. Introduction

π-Conjugated polymers have been extensively investigated as materials for organic photovoltaic (OPV) cells because the solution processing of conjugated polymers enables the large-area fabrication of devices at low costs. Bulk heterojunction (BHJ) solar cells composed of conjugated polymers and fullerene derivatives are of particular interest. Recent advances in this area provide strategies for the molecular designing of high-performance polymers. These strategies include reducing the bandgap of polymers to harvest more sunlight at longer wavelengths and lowering the highest occupied molecular orbital (HOMO) to increase the open circuit voltage (V_{oc}).[1] Side alkyl chains also play crucial roles in the fine tuning of solubility, interchain interactions, and coplanarity of main chains.[2] Furthermore, the molecular weight[3] and purity[4] of conjugated polymers were regarded as important factors affecting the performance of BHJ solar cells.[3–5] To achieve high-purity conjugated polymers, residual impurities derived from catalysts and terminal groups[5] such as Br and Sn should be removed. Purification steps such as treatments of terminal groups, Soxhlet extraction, and size exclusion chromatography have been carried out to reduce the residual impurities.[3–5] Because these extra purification steps lead to increased production costs for OPV materials, an improved synthetic method is required for reducing the quantity of produced impurities, thereby simplifying the purification process. One of the possible ways to achieve this goal is to employ a polycondensation reaction via dehydrohalogenative cross-coupling reactions, so-called direct arylation, instead of conventional polycondensation via cross-coupling reactions.[6–12] Because the polycondensation reaction via direct arylation does not require organometallic monomers such as an organotin monomer, this synthetic protocol does not produce stoichiometric amounts of metal-containing wastes and does not form a metal-substituted terminal group. Moreover, our group developed a phosphine-free Pd catalyst for direct arylation polycondensation,[9] which prevents the formation of defects in the polymers arising from the covalently-bonded phosphine groups.[13] In addition, microwave-assisted direct arylation polycondensation affords high-molecular-weight conjugated polymers.[9e] The high molecular weight of the polymers contributes to the high purity of the polymer owing to the low concentration of terminal groups in such polymers. However, the advantage of this synthetic method in terms of the purity of the polymer has not been sufficiently elucidated until now. Therefore, this research is aimed at proving that direct arylation polycondensation provides highly pure polymers, whose purity contributes to the high performance in OPVs. Towards this aim, a simple conjugated polymer with ethylenedioxythiophene and fluorene units was chosen as the model polymer because the polymer could be synthesized from

Dr. J. Kuwabara, Dr. S. J. Choi, Dr. W. Lu, K. Yamazaki, Prof. T. Kanbara
Tsukuba Research Center for Interdisciplinary Materials Science (TIMS)
Graduate School of Pure and Applied Sciences
University of Tsukuba
Tsukuba 305-8573, Japan
E-mail: kanbara@ims.tsukuba.ac.jp
Dr. T. Yasuda, Dr. L. Han
Organic Thin-Film Solar Cells Group
Photovoltaic Materials Unit
National Institute for Materials Science (NIMS)
Tsukuba, Ibaraki 305-0047, Japan
Prof. S. Kagaya
Graduate School of Science and Engineering for Research
University of Toyama
3190, Gofuku, Toyama 930-8555, Japan

DOI: 10.1002/adfm.201302851

readily available monomers. Herein, we report that an efficient synthetic method can improve the purity and molecular weight of the polymer, leading to an improved OPV performance up to 4% power conversion efficiency (PCE) even though the polymer forms an amorphous film, which absorbed in a limited region of the spectrum.

2. Results and Discussion

2.1. Synthesis

The synthetic scheme and results are summarized in **Scheme 1** and **Table 1**, respectively. A polycondensation reaction via direct C–H arylation of 3,4-ethylenedioxythiophene (**1**) with 2,7-dibromo-9,9-dioctylfluorene (**2**) under microwave heating gave poly[(3,4-ethylenedioxythiophene-2,5-diyl)-(9,9-dioctylfluorene-2,7-diyl)], which had a high molecular weight of 147,000 (**H-PEDOTF**).[9e] A similar reaction under conduction heating gave a relatively low-molecular-weight polymer (47 500), **L-PEDOTF**.[9c] Polycondensation via the Suzuki-Miyaura cross-coupling reaction was conducted for comparison of the obtained polymer with **H-PEDOTF** and **L-PEDOTF**.[14] The reaction conditions for the reaction between 2,5-dibromo-3,4-ethylenedioxythiophene (**3**) and 9,9-dioctylfluorene-2,7-diboronic acid bis(1,3-propanediol) ester (**4**) were optimized for maximizing the molecular weight of the polymer (Supporting Information, Table S1). The reaction using the recently developed Pd precatalyst **5**[15,16] affords the corresponding polymer (**S-PEDOTF**) with a molecular weight of 17 100 which was higher than the reported molecular weight (12 700).[14a] The ^{1}H NMR spectra of all the polymers are essentially identical except for the intensity of the signals from the terminal units (Supporting Information, Figure S1).

2.2. Purity and Physical Properties

Elemental analyses were conducted to evaluate the purity of the polymers (**Table 2**). The experimental data for the composition of C and H for **H-PEDOTF** were in good agreement with the values calculated from the composition of the repeating unit. Moreover, the experimental data showed that the amount of Br in **H-PEDOTF** was lower than the detection limit. It should be noted that **H-PEDOTF** was purified only by washing with several solvents followed by reprecipitation; no other purifications such as treatments of the terminal groups, Soxhlet extraction, and size exclusion chromatography were carried out. Nonetheless, the high purity of the obtained polymers was confirmed by elemental analysis. Since Br was not detected in **H-PEDOTF**, it suggests that the terminal C–Br groups were mostly consumed due to efficient C–C bond formation, which was confirmed by the high degree of polymerization (278) in **H-PEDOTF**. In addition to the consumption of C–Br groups by C–C bond formation, a side debromination reaction might have contributed to the consumption of the Br terminals of the polymer. In contrast to **H-PEDOTF**, the analytical data for **L-PEDOTF** and **S-PEDOTF** showed a relatively large discrepancy in the

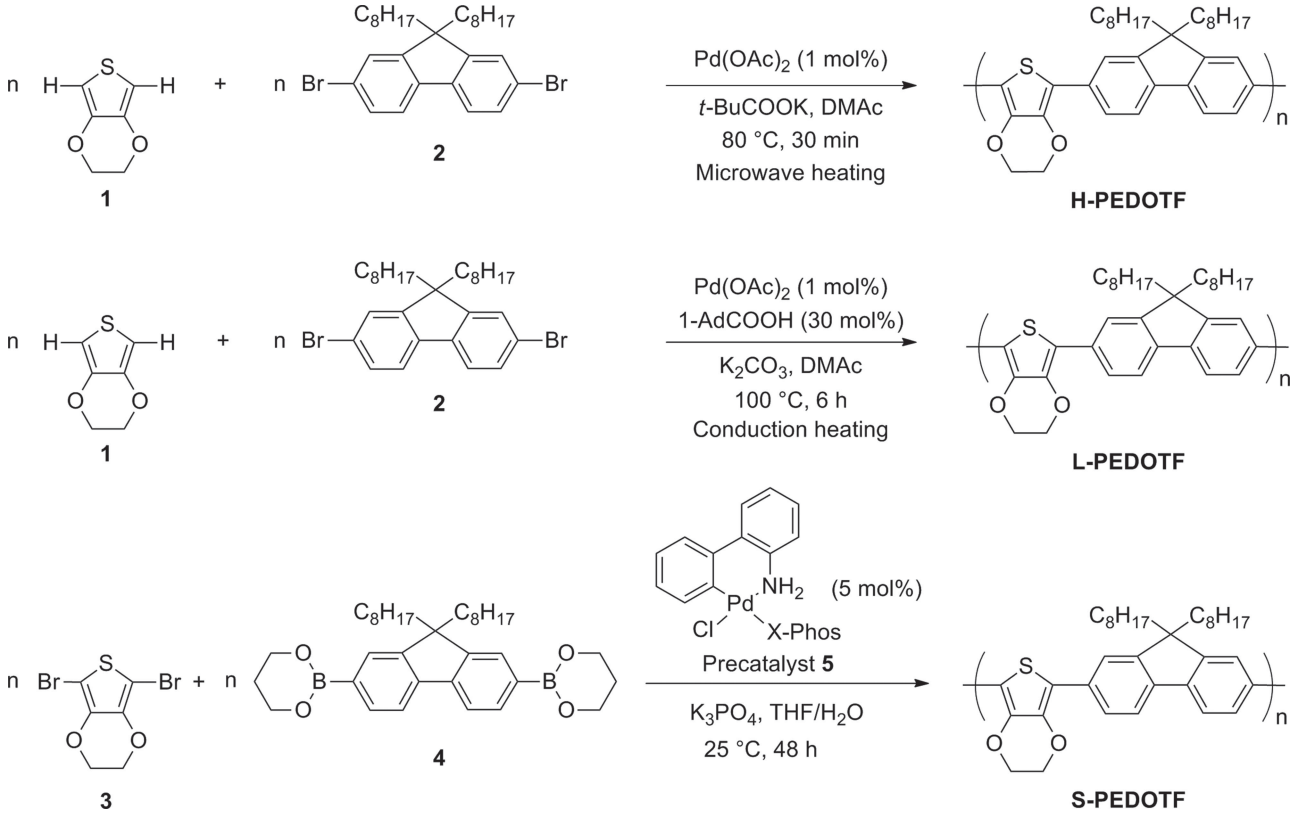

Scheme 1. Synthesis of **PEDOTF** by three different synthetic methods.

Table 1. Results of polycondensation reactions.

Polymer	Bond formation	Heating method	Yield [%]	M_n[a)]	M_w/M_n[a)]	DP[b)]
H-PEDOTF[c)]	Direct arylation	Microwave heating	89	147 000	2.89	278
L-PEDOTF[d)]	Direct arylation	Conduction heating	85	47 500	3.00	90
S-PEDOTF	Suzuki coupling	Conduction heating	85	17 100	2.08	32

[a)]Estimated by GPC calibrated on polystyrene standards; [b)]Degree of polymerization; [c)]Literature;[9e] [d)]Literature.[9c]

Table 2. Results of elemental analysis and ICP-AES.

	Elemental analysis [%]			ICP-AES [ppm]	
	C	H	Br	Pd	P
Calculated value[a)]	79.50	8.39	0		
H-PEDOTF	79.44	8.33	0	1590	nd[b)]
L-PEDOTF	78.52	8.01	0.34	2300	nd[b)]
S-PEDOTF	77.48	8.42	0.08	4390	470

[a)]The values were calculated from the formula of the constituting repeating unit; [b)]Not detected.

composition of C and H. Moreover, residual Br was observed for both **L-PEDOTF** (0.34%) and **S-PEDOTF** (0.08%) presumably owing to incomplete C-C bond formation at the C-Br moiety and untreated terminal Br groups.

MALDI-TOF-MS measurements were conducted for gaining information on the terminal units of the polymers. The MALDI-TOF-MS spectrum of **H-PEDOTF** in the measurable molecular weight range exhibits peaks consistent with an alternating structure containing two hydrogen-terminated groups (Figure S2, Supporting Information), indicating the absence of C–Br terminal units. This result is consistent with the results of elemental analysis. In contrast, the MALDI-TOF-MS spectrum of **L-PEDOTF** exhibits peaks corresponding to a Br-terminated polymer. Finally, the spectrum of **S-PEDOTF** indicates the existence of several types of terminal units and minor quantities of non-alternating structures (Figure S2, Supporting Information).

The inductively coupled plasma-atomic emission spectrometric (ICP-AES) measurements provide information on the residual Pd and P contents in the polymers (Table 2). **H-PEDOTF** and **L-PEDOTF**, which were synthesized with 1 mol% of the Pd precatalyst, contained about 2000 ppm of Pd. Twice the amount of residual Pd (4390 ppm) was observed in **S-PEDOTF**, which was synthesized with 5 mol% of the Pd precatalyst. The residual amount of Pd in the polymer could be reduced by using the efficient synthetic method that required small amounts of the Pd precatalyst. **H-PEDOTF** and **L-PEDOTF** do not contain any phosphorous because phosphine ligands were not used. In contrast, residual P (470 ppm) was observed in **S-PEDOTF**, which originated from the phosphine ligand of the precatalyst. These assessments show the importance of the choice of synthetic method employed in terms of the purity of the obtained polymer and the advantages of direct arylation polycondensation under microwave heating.

The absorption spectra of the polymers were almost identical and the values of optical bandgap were determined to be 2.5 eV (**Figure 1**). Moreover, the highest occupied molecular orbital (HOMO) levels of the three polymers were located at a similar value of about –5.2 eV, as determind by photoelectron yield spectroscopy (PYS) of the polymer films. These results indicated that the energy level was independent of molecular weight or purity of the polymers. Atomic force microscopy (AFM) images of the spin-coated thin films of the polymers exhibited flat surfaces in all cases, which were characteristic of amorphous polymers (Figure S3, Supporting Information).

2.3. OFET and OPV Performance

To evaluate the carrier mobilities of the polymers, organic field-effect transistors (OFETs) were fabricated using the polymers. Although the OFET measurements provided information on carrier mobilities in a direction parallel to the substrate, the measurements were also helpful for estimating the carrier mobilities in a direction perpendicular to the substrate in OPV cells, especially when amorphous polymers were used as the active materials. The results of the measurements are shown in **Figure 2** and **Table 3**. The OFET with **H-PEDOTF** exhibited a field-effect hole mobility of $1.2 \pm 0.1 \times 10^{-3}$ cm^2 V^{-1} s^{-1} (average value with standard error calculated from the results of six OFET samples), which was higher than that of **S-PEDOTF** ($3.2 \pm 0.2 \times 10^{-5}$ cm^2 V^{-1} s^{-1}) by two orders of magnitude.

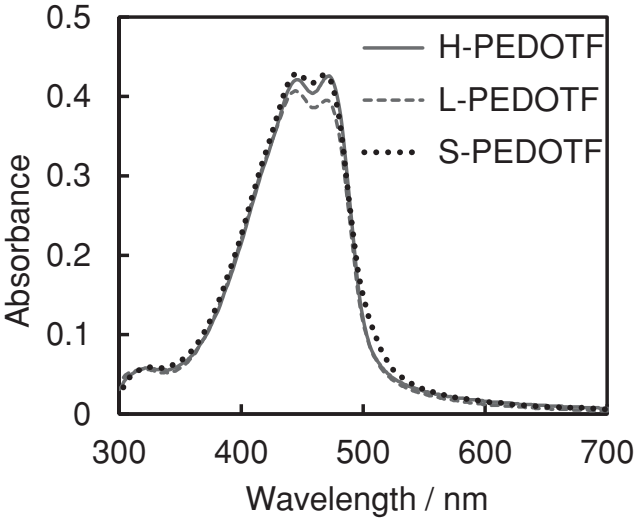

Figure 1. UV-Vis absorption spectra of the polymers in the thin-film state; the thicknesses of the films are 32 nm for **H-PEDOTF**, 30 nm for **L-PEDOTF**, and 33 nm for **S-PEDOTF**.

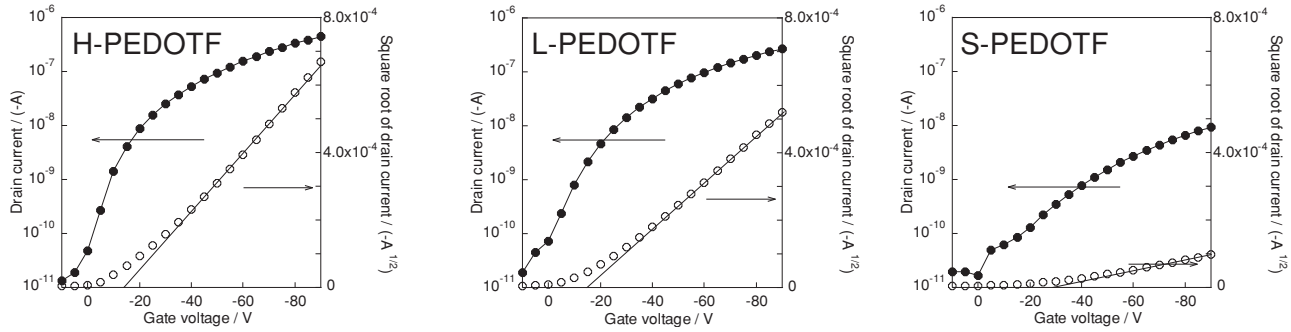

Figure 2. Typical transfer characteristics (measured at drain voltage of −100 V) of the top-contact OFETs for **H-PEDOTF**, **L-PEDOTF**, and **S-PEDOTF** films spin-coated from *o*-DCB solution and annealed for 10 min at 110 °C.

Table 3. OFET[a] characteristics.

Polymer	μ_h[b] [$cm^2 V^{-1} s^{-1}$]	on/off ratio	V_{th}[c] [V]
H-PEDOTF	$1.2 \pm 0.1 \times 10^{-3}$	$1.6 \pm 0.4 \times 10^4$	−18 ± 1
L-PEDOTF	$7.7 \pm 0.4 \times 10^{-4}$	$9.2 \pm 0.2 \times 10^3$	−21 ± 1
S-PEDOTF	$3.2 \pm 0.2 \times 10^{-5}$	$4.3 \pm 1.0 \times 10^2$	−30 ± 1

[a]The average value with standard error were calculated from the results of six or more OFET samples. OFET configuration; Glass/Au gate electrode/Parylene-C insulator/Polymer/Au source-drain electrodes; [b]Field-effect hole mobility; [c]Threshold voltage.

Compared to **L-PEDOTF** ($7.7 \pm 0.4 \times 10^{-4}$ cm^2 V^{-1} s^{-1}), higher values of hole mobility were reproducibly observed for OFETs fabricated using **H-PEDOTF**. The high purity of **H-PEDOTF** is likely to be the origin of high hole mobility and on/off ratio because impurities present in materials act as carrier traps.[4] The high molecular weight of **H-PEDOTF** should also contribute to the good performance of **H-PEDOTF**-based OFETs owing to the presence of only a small amount of terminal units because the terminal units are regarded as a defect of polymer material.[3] It has been reported that a polymer with a similar structure (M_n of 16 620) but with an alkyl side chain different from that in **PEDOTF**, did not exhibit an FET behavior.[14b] These facts show that the high purity and molecular weight of polymers play a crucial role in realizing the maximum potential of such polymers, which act as optoelectronic materials.

To study the effects of purity and molecular weight of the polymers on OPV characteristics, OPV cells were prepared from 1:4 blends of the polymers with $PC_{60}BM$ or $PC_{70}BM$ (See experimental section and Supporting Information). An OPV cell with an active layer of **H-PEDOTF**:$PC_{60}BM$ afforded a PCE of 1.88%, which was a relatively high value for a polymer material with an absorption wavelength below 500 nm (Table S2, Supporting Information).[1a–d,17] When $PC_{70}BM$ was used instead of $PC_{60}BM$, the value of the short-circuit current density (J_{sc}) was significantly improved (**Table 4**) and incident photon to current conversion was observed at wavelengths longer than 500 nm (**Figure 3**) because $PC_{70}BM$ has an absorption stronger than that of $PC_{60}BM$ in the visible region from 400 to 700 nm. The good reproducibility of the results was confirmed, as listed in Table S3, Supporting Information. It is important to note that a PCE value of 4% was achieved with a polymer which absorbed in a limited region of the spectrum, as shown in Figure 1. This result strongly suggested the importance of the high molecular weight and high purity of the polymers. In sharp contrast, the PCE values of OPV cells prepared using **L-PEDOTF**:$PC_{70}BM$ and **S-PEDOTF**:$PC_{70}BM$ were only 2.55% and 0.48%, respectively. The respective incident photon to current conversion efficiencies (IPCEs) were 73%, 56%, and 27% for **H-PEDOTF**-, **L-PEDOTF**-, and **S-PEDOTF**-based OPVs at a wavelength of 410 nm. The thicknesses of BHJ layers were almost the same: 134 nm for **H-PEDOTF**-, 126 nm for **L-PEDOTF**- and 138 nm for **S-PEDOTF**-based OPV. Therefore, the internal quantum efficiencies (IQEs) of the three OPVs should exhibit the same trend for the values of IPCEs. OPVs using PEDOTFs:$PC_{60}BM$ (1:4) exhibited the same trend as those using PEDOTFs:$PC_{70}BM$ (1:4): PCEs increased in the following order, **H-**, **L-**, and **S-PEDOTF** (Table S2, Supporting Information). The two possible origins for the observed variation in PCEs and IPCEs between the three PEDOTF-based OPVs are as follows: I) the dependency of molecular weight on the morphology of the BHJ layers, and II) the effect of impurities present in PEDOTFs on the hole mobilities and recombination processes in BHJ OPVs.

Table 4. OPV[a] characteristics.

BHJ layer	Solvent	Annealing temp. [°C]	J_{sc}[b] [$mAcm^{-2}$]	V_{oc}[b] [V]	FF[b]	PCE[b] [%]
H-PEDOTF:$PC_{70}BM$	*o*-DCB	110	9.41	0.83	0.52	4.08
H-PEDOTF:$PC_{70}BM$	$CHCl_3$	60	10.18	0.84	0.48	4.04
L-PEDOTF:$PC_{70}BM$	*o*-DCB	110	7.65	0.78	0.42	2.55
S-PEDOTF:$PC_{70}BM$	*o*-DCB	110	2.58	0.59	0.31	0.48

[a]OPV configuration; ITO/PEDOT:PSS (40 nm)/Polymer:$PC_{70}BM$ (1:4) /LiF (1 nm)/Al (80 nm). Illuminated at 100 mW cm^{-2} of AM 1.5; [b]Average values at least two runs.

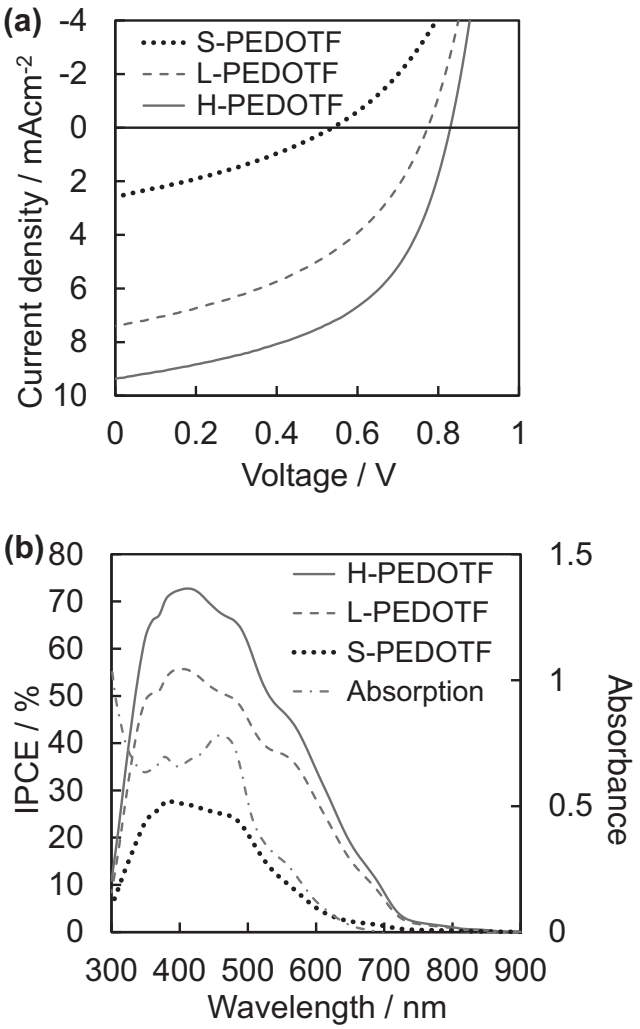

Figure 3. a) Current density-voltage characteristics of Polymer:$PC_{70}BM$ (1:4) BHJ solar cells under AM1.5G illumination; b) IPCEs of the corresponding cells and absorption spectrum of the **H-PEDOTF**:$PC_{70}BM$ (1:4) blend film.

It has been reported that the differences in the molecular weight of the polymers affected the phase morphology of a BHJ mixture, thereby affecting the charge separation and mobility.[3] However, no obvious difference was observed in the AFM images of the three types of PEDOTF:$PC_{70}BM$ (1:4) films (**Figure 4**) and PEDOTF:$PC_{60}BM$ (1:4) films (Figure S4, Supporting Information). Two OPVs based on BHJ layers of **H-PEDOTF**:$PC_{70}BM$ (1:4) were fabricated under significantly different fabrication conditions. One BHJ layer was fabricated using chloroform ($CHCl_3$, boiling point 61 °C) solution and annealed at 60 °C for 10 min, whereas the other BHJ layer was fabricated using *o*-dichlorobenzene (*o*-DCB, boiling point 181 °C) solution, and annealed at 110 °C for 10 min. Interestingly, similar film morphologies (Figure 4c,d) and PCEs (Table 4) were observed for both the OPVs despite being fabricated under significantly different conditions. Therefore, these results indicate that the morphology of the BHJ layers was independent of the molecular weight of the polymers and fabrication conditions, presumably due to the amorphous nature of PEDOTF.[18] This result rules out the dependence of molecular weight on the morphlogy of the BHJ layers as a possible origin for the observed variation in PCEs and IPCEs between the three PEDOTF-based OPVs. Next, we investigated the effect of impurities present in PEDOTFs on the hole mobilities and recombination in BHJ OPVs. The chemical impurities in materials, which mainly consist of a Pd-based derivative and a terminal group, are well known for affecting the performance of BHJ OPVs in a variety of ways.[3,4] For example, such impurities can decrease the carrier mobility and act as traps that increase the probability of charge recombination. The improved performance of **H-PEDOTF**-based OPVs is mainly attributed to the high carrier mobility of the polymer compared to the other polymers. In general, an enhancement in the carrier mobility of a polymer increases the values of J_{sc} and fill factor (*FF*).[1] Indeed, these values listed in Table 4 increased with increasing hole mobility. To gain further information on the effect of impurities present in PEDOTFs on the performance of BHJ OPVs, we investigated the dependence of V_{oc} on the light intensity. This investigation provides information on the details of the recombination process because all photogenerated carriers recombine within the cell ($J = 0$ at V_{oc}). Trap-assisted and bimolecular recombination are considered to be the main recombination mechanisms operating in BHJ OPVs.[19] In the case of trap-assisted recombination, the slope of V_{oc} in the plot of V_{oc} versus the natural logarithm of the light intensity equals $2kT/e$, where k is the Boltzmann coefficient, T is the absolute temperature (in this study, 299 K), and e is the elementary charge. On the other hand, a slope equal to kT/e is observed in

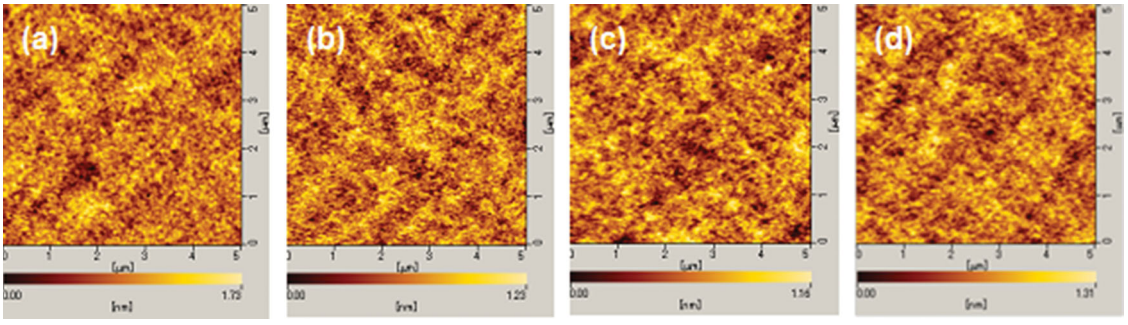

Figure 4. AFM images (5 μm × 5 μm) of a) **S-PEDOTF**:$PC_{70}BM$ (1:4), b) **L-PEDOTF**:$PC_{70}BM$ (1:4), and c) **H-PEDOTF**:$PC_{70}BM$ (1:4) films fabricated by spin coating from *o*-DCB (annealed at 110 °C for 10 min) and d) **H-PEDOTF**:$PC_{70}BM$ (1:4) films fabricated by spin coating from $CHCl_3$ (annealed at 60 °C for 10 min).

the case of bimolecular recombination. **S-PEDOTF**-based OPV exhibits a stronger dependence of V_{oc} on light intensity, with a slope of 1.78 kT/e, as compared to a slope of 1.47 kT/e for **H-PEDOTF**-based OPVs (Figure S5, Supporting Information). This result indicates that trap-assisted recombination is mainly responsible for the loss of photocarriers in **S-PEDOTF**-based OPVs. It is apparent that an increase in the impurities present in the OPVs introduces more trap sites, thereby reducing the values of $V_{oc}J_{sc}$, and FF and causing a significant decrease in the PCE. The results on OPV characteristics confirm that both high molecular weight and purity of the polymers obtained from direct arylation polycondensation lead to a high performance in OPVs. As the impurities can also be chemically reactive and limit the device lifetime, we measured the lifetime of OPVs in preliminary experiments. The results showed that the **H-PEDOTF**-based OPV had a longer lifetime under continuous AM1.5 irradiation compared to the **S-PEDOTF**-based OPV (Figure S6, Supporting Information). Detailed studies on the OPV lifetime are underway.

3. Conclusion

Microwave-assisted direct arylation polycondensation was able to afford a pure and high-molecular-weight polymer even with a simple purification step. This methodology significantly reduces the number of purification steps required for obtaining high-quality polymers. The high purity and molecular weight of the polymer were reflected in the high carrier mobility leading to an improved OPV performance. PCE values of 4% were obtained for the device fabricated with the model polymer. Because this synthetic method can bring out the maximum potential of polymer materials, the application of this synthetic protocol to a well-designed polymer with energy levels appropriate for OPV is expected to give rise to outstanding OPV performances. This methodology shows promise for the efficient synthesis of OPV materials.

4. Experimental Section

3,4-Ethylenedioxythiophene, 2,7-dibromo-9,9-dioctylfluorene, palladium acetate ($Pd(OAc)_2$), and potassium carbonate (K_2CO_3) were received from commercial suppliers and used without further purification. Anhydrous dimethylacetamide (DMAc) was purchased from Kanto Chemical and used as a dry solvent. Pd precatalyst **5**[15] and **L-PEDOTF**[9c] was prepared using a previously reported method. Poly(3,4-ethylenedioxythiophene)-poly(styrenesulfonate) (PEDOT:PSS, CLEVIOS P VP AI 4083) was purchased from Heraeus. $PC_{60}BM$ and $PC_{70}BM$ (purity 99%) were purchased from Solenne. Standard solutions of Pd and P (1000 mg L^{-1}) were purchased from Kanto Chemical.

^1H and $^{13}C\{^1H\}$ NMR spectra were recorded using a Bruker AVANCE-400 NMR spectrometer and Bruker AVANCE-600 NMR spectrometer, respectively. ^1H and $^{13}C\{^1H\}$ NMR spectra were measured using tetramethylsilane (TMS) as the internal standard. Gel permeation chromatography (GPC) measurements were carried out using a SHIMADZU prominence GPC system equipped with polystyrene gel columns, using $CHCl_3$ as the eluent after calibration with polystyrene standards. All the manipulations for the reactions were carried out under a nitrogen atmosphere using a glove box or standard Schlenk technique. MALDI-TOF-MS spectra were recorded using AB SCIEX MALDI TOF/TOF 5800 and dithranol as the matrix. The HOMO energy levels were estimated by PYS using an AC-3 spectrometer (Riken Keiki). Ultraviolet-visible (UV-vis) absorption spectra were recorded using a U-3010 spectrometer (Hitachi). The amounts of residual Pd and P in the polymers were determined by ICP-AES using a Perkin Elmer Optima 7300DV inductively coupled plasma atomic emission spectrometer after decomposing the weighed samples in analytical grade nitric acid with heating.

Synthesis of ***H-PEDOTF***:[9e] $Pd(OAc)_2$ (1.1 mg, 0.0050 mmol), and 2,7-dibromo-9,9-dioctylfluorene (274 mg, 0.50 mmol) were weighed in air and placed in a 10-mL microwave vessel with a magnetic stir bar. The vessel was transferred to a glove box under nitrogen atmosphere. Next, potassium pivalate (175 mg, 1.3 mmol), 3,4-ethylenedioxythiophene (53.4 µL, 0.50 mmol), and degassed DMAc (5 mL) were added. The vessel was sealed with a septum and removed from the glove box. The sealed vessel was then placed in the microwave reactor and heated at 80 °C for 30 min. After cooling to room temperature, an aqueous solution of ethylenediaminetetraacetic acid disodium salt (pH = 8) was added. The suspension was stirred for 2 h at room temperature. The precipitate was separated by filtration and washed with 0.1 M HCl solution, distilled water, methanol, and hexane. The precipitate was dissolved in $CHCl_3$, and the solution was filtered through Celite to remove insoluble materials. Reprecipitation from a chloroform/methanol mixture afforded the polymer as a pale yellow solid. The product was washed with *N,N′*-dimethylformamide (DMF) and methanol. **H-PEDOTF** with a molecular weight of 147 000 (M_w/M_n = 2.89) was obtained in 89% yield. ^1H NMR (400 MHz, $CDCl_3$, δ): 7.82 (d, J = 8 Hz, 2H), 7.71–7.70 (m, 4H), 4.45 (s, 4H), 2.06 (br, 4H), 1.22–1.10 (m, 20H), 0.82–0.80 (m, 6H), 0.76 (br, 4H).

Synthesis of ***S-PEDOTF***: A mixture of Pd precatalyst **5** (19.7 mg, 0.025 mmol), K_3PO_4 (2.12 g, 10 mmol), 9,9-dioctylfluorene-2,7-diboronic acid bis(1,3-propanediol) ester (279 mg, 0.50 mmol), 2,5-dibromo-3,4-ethylenedioxythiophene (150 mg, 0.50 mmol) was stirred in a mixture of THF (2.5 mL) and H_2O for 48 h at 25 °C under a nitrogen atmosphere. An aqueous solution of ethylenediaminetetraacetic acid disodium salt (pH = 8) was added. The suspension was stirred for 2 h at room temperature. The precipitate was separated by filtration and washed with 1 M HCl solution, distilled water, methanol, and hexane. The precipitate was then dissolved in $CHCl_3$ and the solution was filtered through Celite to remove insoluble materials. Reprecipitation from a chloroform/methanol mixture afforded the polymer as a pale yellow solid. The product was washed with DMF and methanol. **S-PEDOTF** with a molecular weight of 17 100 (M_w/M_n = 2.08) was obtained in 85% yield.

Fabrication and Characterization of OFETs: To estimate the hole mobilities of the PEDOTFs, OFETs with a top-contact geometry were fabricated and characterized as follows. A glass/Au gate electrode/Parylene-C insulator substrate was prepared according to the previously reported methods.[20] The PEDOTFs were spin-coated from *o*-dichlorobenzene (*o*-DCB, boiling point 181 °C) solution onto the Parylene-C layer. The coated substrate was then transferred to a N_2-filled glove box where it was dried for 10 min at 110 °C. Au (40 nm) source-drain electrodes were thermally evaporated onto the substrates through shadow masks. The channel length and width were fixed at 75 µm and 5 mm, respectively. The OFET measurements were conducted using a Keithley 2636A System Source Meter under vacuum.

Fabrication and Characterization of OPV Cells: The OPV cells were fabricated in the following configuration: ITO/PEDOT:PSS/BHJ layer/LiF/Al. The patterned ITO (conductivity: 10 Ω/square) glass was precleaned in an ultrasonic bath of acetone and ethanol and then treated in an ultraviolet-ozone chamber. A thin layer (40 nm) of PEDOT:PSS was spin-coated onto the ITO at 3000 rpm and air-dried at 110 °C for 10 min on a hot plate. The substrate was then transferred to a N_2-filled glove box where it was re-dried at 110 °C for 10 min on a hot plate. An *o*-DCB solution of the PEDOTFs and $PC_{60}BM$ or $PC_{70}BM$ blended in a 1:4 ratio was subsequently spin-coated onto the PEDOT:PSS surface to form the BHJ layer. The substrates with the BHJ layers were dried for 10 min at 110 °C for the film spin-cast using the *o*-DCB solution. LiF (1 nm) and Al (80 nm) were then deposited onto the active layer by conventional thermal evaporation at a chamber pressure lower than 5×10^{-4} Pa, which provided the devices with an active area of 2 mm × 2 mm. The thicknesses of BHJ and PEDOT:PSS layers were measured

using an automatic microfigure measuring instrument (SURFCORDER ET200, Kosaka Laboratory, Ltd.). The current density-voltage (*J–V*) curves were measured using an ADCMT 6244 DC voltage current source/monitor under AM 1.5 solar-simulated light irradiation of 100 mW cm^{-2} (OTENTO-SUN III, Bunkoh-Keiki Co.). The incident photon to current conversion efficiency (IPCE) was measured using a SM-250 system (Bunkoh-Keiki Co.). As a part of the structural characterizations, the surface morphologies were studied using atomic force microscopy (AFM, Nanocute, SII Nano Technology, Inc.).

Supporting Information

Supporting Information is available from the Wiley Online Library or from the author.

Acknowledgements

The authors thank the Chemical Analysis Center of University of Tsukuba for the measurements of NMR spectra and MALDI-TOF-MS. The authors also thank to Prof. T. Koizumi and the Center for Advanced Materials Analysis, Technical Department, Tokyo Institute of Technology for the elemental analyses. This work was supported by the Collaborative Research Program of Institute for Chemical Research, Kyoto University and Industrial Technology Research Grant Program in 2011 from New Energy and Industrial Technology Development Organization (NEDO) of Japan, and was partly supported by Grants-in-Aids for Scientific Resaerch (25288052) and Challenging Exploratory Research (25620096).

Received: August 14, 2013
Revised: October 14, 2013
Published online: February 12, 2014

[1] a) M. C. Scharber, D. Mühlbacher, M. Koppe, P. Denk, C. Waldauf, A. J. Heeger, C. J. Brabec, *Adv. Mater.* **2006**, *18*, 789; b) Y.-J. Cheng, S-H. Yang, C-S. Hsu, *Chem. Rev.* **2009**, *109*, 5868; c) P.-L. T. Boudreault, A. Najari, M. Leclerc, *Chem. Mater.* **2011**, *23*, 456; d) R. S. Kularatne, H. D. Magurudeniya, P. Sista, M. C. Biewer, M. C. Stefan, *J. Polym. Sci. Part A: Polym. Chem.* **2013**, *51*, 743; e) J. You, L. Dou, K. Yoshimura, T. Kato, K. Ohya, T. Moriarty, K. Emery, C.-C. Chen, J. Gao, G. Li, Y. Yang, *Nat. Commun.* **2013**, *4*, 1446.

[2] a) H. Zhou, L. Yang, S. Xiao, S. Liu, W. You, *Macromolecules* **2010**, *43*, 811; b) Q. Shi, H. Fan, Y. Liu, J. Chen, L. Ma, W. Hu, Z. Shuai, Y. Li, X. Zhan, *Macromolecules* **2011**, *44*, 4230; c) H. Bronstein, D. S. Leem, R. Hamilton, P. Woebkenberg, S. King, W. Zhang, R. S. Ashraf, M. Heeney, T. D. Anthopoulos, J. de Mello, I. McCulloch, *Macromolecules* **2011**, *44*, 6649; d) R. L. Uy, S. C. Price, W. You, *Macromol. Rapid Commun.* **2012**, *33*, 1162; e) H. Zhou, L. Yang, W. You, *Macromolecules* **2012**, *45*, 607; f) I. McCulloch, R. S. Ashraf, L. Biniek, H. Bronstein, C. Combe, J. E. Donaghey, D. I. James, C. B. Nielsen, B. C. Schroeder, W. Zhang, *Acc. Chem. Res.* **2012**, *45*, 714; g) A. Marrocchi, D. Lanari, A. Facchetti, L. Vaccaro, *Energy Environ. Sci.* **2012**, *5*, 8457.

[3] a) M. Tong, S. Cho, J. T. Rogers, K. Schmidt, B. B. Y. Hsu, D. Moses, R. C. Coffin, E. J. Kramer, G. C. Bazan, A. J. Heeger, *Adv. Funct. Mater.* **2010**, *20*, 3959; b) T.-Y. Chu, J. Lu, S. Beaupré, Y. Zhang, J.-R. Pouliot, J. Zhou, A. Najari, M. Leclerc, Y. Tao, *Adv. Funct. Mater.* **2012**, *22*, 2345; c) I. Osaka, M. Saito, H. Mori, T. Koganezawa, K. Takimiya, *Adv. Mater.* **2012**, *24*, 425; d) R. S. Ashraf, B. C. Schroeder, H. A. Bronstein, Z. Huang, S. Thomas, R. J. Kline, C. J. Brabec, P. Rannou, T. D. Anthopoulos, J. R. Durrant, I. McCulloch, *Adv. Mater.* **2013**, *25*, 2029.

[4] a) F. C. Krebs, R. B. Nyberg, M. Jørgensen, *Chem. Mater.* **2004**, *16*, 1313; b) P. A. Troshin, D. K. Susarova, Y. L. Moskvin, I. E. Kuznetsov, S. A. Ponomarenko, E. N. Myshkovskaya, K. A. Zakharcheva, A. A. Balakai, S. D. Babenko, V. F. Razumov, *Adv. Funct. Mater.* **2010**, *20*, 4351; c) J. Kettle, M. Horie, L. A. Majewski, B. R. Saunders, S. Tuladhar, J. Nelson, M. L. Turner, *Sol. Energy Mater. Sol. Cells* **2011**, *95*, 2186; d) N. Camaioni, F. Tinti, L. Franco, M. Fabris, A. Toffoletti, M. Ruzzi, L. Montanari, L. Bonoldi, A. Pellegrino, A. Calabrese, R. Po, *Org. Electron.* **2012**, *13*, 550; e) S. V. Mierloo, A. Hadipour, M.-J. Spijkman, N. V. den Brande, B. Ruttens, J. Kesters, J. D'Haen, G. V. Assche, D. M. de Leeuw, T. Aernouts, J. Manca, L. Lutsen, D. J. Vanderzande, W. Maes, *Chem. Mater.* **2012**, *24*, 587; f) M. P. Nikiforov, B. Lai, W. Chen, S. Chen, R. D. Schaller, J. Strzalka, J. Maser, S. B. Darling, *Energy Environ. Sci.* **2013**, *6*, 1513.

[5] a) Y. Kim, S. Cook, J. Kirkpatrick, J. Nelson, J. R. Durrant, D. D. C. Bradley, M. Giles, M. Heeney, R. Hamilton, I. McCulloch, *J. Phys. Chem. C* **2007**, *111*, 8137; b) J. K. Park, J. Jo, J. H. Seo, J. S. Moon, Y. D. Park, K. Lee, A. J. Heeger, G. C. Bazan, *Adv. Mater.* **2011**, *23*, 2430; c) C. Duan, F. Huang, Y. Cao, *J. Mater. Chem.* **2012**, *22*, 10416.

[6] a) A. Facchetti, L. Vaccaro, A. Marrocchi, *Angew. Chem., Int. Ed.* **2012**, *51*, 3520; b) S. Kowalski, S. Allard, K. Zilberberg, T. Riedl, U. Scherf, *Prog. Polym. Sci.* **2013**, *38*, 1805; c) P. P. Khlyabich, B. Burkhart, A. E. Rudenko, B. C. Thompson, *Polymer* **2013**, *54*, 5267; d) K. Okamoto, J. Zhang, J. B. Housekeeper, S. R. Marder, C. K. Luscombe, *Macromolecules* **2013**, *46*, 8059.

[7] a) Q. Wang, R. Takita, Y. Kikuzaki, F. Ozawa, *J. Am. Chem. Soc.* **2010**, *132*, 11420; b) Q. Wang, M. Wakioka, F. Ozawa, *Macromol. Rapid Commun.* **2012**, *33*, 1203; c) M. Wakioka, Y. Kitano, F. Ozawa, *Macromolecules* **2013**, *46*, 370.

[8] a) W. Lu, J. Kuwabara, T. Kanbara, *Macromolecules* **2011**, *44*, 1252; b) W. Lu, J. Kuwabara, T. Iijima, H. Higashimura, H. Hayashi, T. Kanbara, *Macromolecules* **2012**, *45*, 4128.

[9] a) Y. Fujinami, J. Kuwabara, W. Lu, H. Hayashi, T. Kanbara, *ACS Macro Lett.* **2012**, *1*, 67; b) W. Lu, J. Kuwabara, T. Kanbara, *Polym. Chem.* **2012**, *3*, 3217; c) K. Yamazaki, J. Kuwabara, T. Kanbara, *Macromol. Rapid Commun.* **2013**, *34*, 69; d) J. Kuwabara, Y. Nohara, S. J. Choi, Y. Fujinami, W. Lu, K. Yoshimura, J. Oguma, K. Suenobu, T. Kanbara, *Polym. Chem.* **2013**, *4*, 947; e) S. J. Choi, J. Kuwabara, T. Kanbara, *ACS Sustainable Chem. Eng.* **2013**, *1*, 878.

[10] a) P. Berrouard, A. Najari, A. Pron, D. Gendron, P.-O. Morin, J.-R. Pouliot, J. Veilleux, M. Leclerc, *Angew. Chem., Int. Ed.* **2012**, *51*, 2068; b) S. Beaupré, A. Pron, S. H. Drouin, A. Najari, L. G. Mercier, A. Robitaille, M. Leclerc, *Macromolecules* **2012**, *45*, 6906; c) P. Berrouard, S. Dufresne, A. Pron, J. Veilleux, M. Leclerc, *J. Org. Chem.* **2012**, *77*, 8167; d) N. Allard, A. Najari, J.-R. Pouliot, A. Pron, F. Grenier, M. Leclerc, *Polym. Chem.* **2012**, *3*, 2875; e) L. G. Mercier, M. Leclerc, *Acc. Chem. Res.* **2013**, *46*, 1597.

[11] a) A. Kumar, A. Kumar, *Polym. Chem.* **2010**, *1*, 286; b) S. Kowalski, S. Allard, U. Scherf, *ACS Macro Lett.* **2012**, *1*, 465; c) A. E. Rudenko, C. A. Wiley, S. M. Stone, J. F. Tannaci, B. C. Thompson, *J. Polym. Sci. Part A: Polym. Chem.* **2012**, *50*, 3691; d) S.-W. Chang, H. Waters, J. Kettle, Z.-R. Kuo, C.-H. Li, C.-Y. Yu, M. Horie, *Macromol. Rapid Commun.* **2012**, *33*, 1927; e) K. Okamoto, J. B. Housekeeper, F. E. Michael, C. K. Luscombe, *Polym. Chem.* **2013**, *4*, 3499; f) L. A. Estrada, J. J. Deininger, G. D. Kamenov, J. R. Reynolds, *ACS Macro Lett.* **2013***2*, 869.

[12] A. Mori and colleagues reported C–H functionalization polycondensation of 2–halo–3–alkylthiophenes using magnesium amide for a deprotonation. a) S. Tamba, K. Shono, A. Sugie, A. Mori, *J. Am. Chem. Soc.* **2011**, *133*, 9700; b) S. Tamba, S. Tanaka, Y. Okubo, H. Meguro, S. Okamoto, A. Mori, *Chem. Lett.* **2011**, *40*, 398; c) S. Tamba, S. Mitsuda, F. Tanaka, A. Sugie, A. Mori, *Organometallics* **2012**, *31*, 2263.

[13] a) J. Frahn, B. Karakaya, A. Schäfer, A.-D. Schlűter, *Tetrahedron* **1997**, *53*, 15459; b) F. E. Goodson, T. I. Wallow, B. M. Novak, *Macromolecules* **1998**, *31*, 2047; c) F. E. Goodson, S. I. Hauck, J. F. Hartwig, *J. Am. Chem. Soc.* **1999**, *121*, 7527.

[14] a) A. Donat-Bouillud, I. Lévesque, Y. Tao, M. D'Iorio, S. Beaupré, P. Blondin, M. Ranger, J. Bouchard, M. Leclerc, *Chem. Mater.* **2000**, *12*, 1931; b) Z. Li, Y. Zhang, A. L. Holt, B. P. Kolasa, J. G. Wehner, A. Hampp, G. C. Bazan, T.-Q. Nguyen, D. E. Morse, *New J. Chem.* **2011**, *35*, 1327.

[15] a) T. Kinzel, Y. Zhang, S. L. Buchwald, *J. Am. Chem. Soc.* **2010**, *132*, 14073; b) N. C. Bruno, M. T. Tudge, S. L. Buchwald, *Chem. Sci.* **2013**, *4*, 916.

[16] H.-H. Zhang, C.-H. Xing, G. B. Tsemo, Q.-S. Hu, *ACS Macro Lett.* **2013**, *2*, 10.

[17] a) G. L. Schulz, X. Chen, S. Holdcroft, *Appl. Phys. Lett.* **2009**, *94*, 023302; b) T. Yasuda, T. Suzuki, M. Takahashi, L. Han, *Sol. Energy Mater. Sol. Cells* **2011**, *95*, 3509; c) T. Yasuda, K. Yonezawa, M. Ito, H. Kamioka, L. Han, Y. Morimoto, *J. Photopolym. Sci. Technol.* **2012**, *25*, 271.

[18] a) T. Yasuda, Y. Shinohara, T. Ishi-i, L. Han, *Org. Electron.* **2012**, *13*, 1802; b) T. Yasuda, Y. Shinohara, T. Matsuda, L. Han, T. Ishi-i, *J. Polym. Sci. Part A: Polym. Chem.* **2013**, *51*, 2536.

[19] a) S. R. Cowan, A. Roy, A. J. Heeger, *Phys. Rev. B* **2010**, *82*, 245207; b) S. R. Cowan, W. L. Leong, N. Banerji, G. Dennler, A. J. Heeger, *Adv. Funct. Mater.* **2011**, *21*, 3083; c) W. L. Leong, G. C. Welch, L. G. Kaake, C. J. Takacs, Y. Sun, G. C. Bazan, A. J. Heeger, *Chem. Sci.* **2012**, *3*, 2103.

[20] H. Nagashima, M. Saito, H. Nakamura, T. Yasuda, T. Tsutsui, *Org. Electron.* **2010**, *11*, 658.